J Appl Electrochem (2013) 43:533–540
DOI 10.1007/s10800-013-0537-2

ORIGINAL PAPER

Electrochemical characterization of anodic biofilm development in a microbial fuel cell

Edith Martin · Oumarou Savadogo · Serge R. Guiot · Boris Tartakovsky

Received: 26 October 2012 / Accepted: 11 February 2013 / Published online: 26 February 2013

Abstract Electrochemical impedance spectroscopy, cyclic voltammetry, and polarization tests were used to monitor the progress of the anode colonization by electrode-reducing microorganisms in a single-chamber membraneless microbial fuel cell seeded with anaerobic sludge. The electrochemical methods showed that an increase in microbial fuel cell power output coincided with a progressive decrease of the anode internal resistance and a more negative open circuit potential. Two redox systems were observed in cyclic voltammograms shortly after microbial fuel cell startup, while a redox system with a peak around −330 mV (vs. Ag/AgCl) was predominant in the mature biofilm. The redox systems were also dependent on the external resistance chosen for microbial fuel cell operation. This suggests that within the diverse microbial populations several species are capable of electron transfer to the anode, and that the microorganisms with the highest electron transfer rate become predominant. Furthermore, the growth of these electrode-reducing microorganisms can be accelerated by optimizing the microbial fuel cell electrical load.

Keywords MFC · Anodic biofilm · Cyclic voltammetry · EIS · Internal resistance

E. Martin · O. Savadogo
Laboratory of Electrochemistry and Energetic Materials, École Polytechnique de Montréal, Centre-ville, C.P. 6079, Montreal, QC H3C 3A7, Canada

E. Martin · S. R. Guiot · B. Tartakovsky (✉)
National Research Council of Canada (NRC-EME), 6100 Royalmount Avenue, Montreal, QC H4P 2A2, Canada
e-mail: boris.tartakovsky@cnrc-nrc.gc.ca

1 Introduction

Electricity production in microbial fuel cells (MFCs) relies on microorganisms transferring electrons to the anode through a conductive biofilm matrix, by direct contact with the electrode or by self-produced mediators [1–3]. Upon MFC inoculation, the anode-reducing microorganisms colonize the anode surface forming a biofilm [4, 5]. The rate of biofilm formation and its composition in a MFC seeded with a mixed microbial population depends on a number of factors including operating conditions such as organic load and external resistance [6, 7]. A better understanding of how the anodophilic biofilm is formed can be achieved using electrochemical techniques such as polarization tests (PTs), cyclic voltammetry (CV), and electrochemical impedance spectroscopy (EIS) [8–10].

PTs are used by almost every MFC study [11–16] since it provides a simple and convenient tool for comparison between various MFC designs and operating conditions. Polarization and power curves obtained in a PT can be used to measure open circuit voltage (OCV), estimate total internal resistance and the maximal power output of a MFC [17]. Electrode potential measurements against a reference electrode during a PT can be used to estimate anode and cathode resistance. However, resistance estimations obtained using the PT technique are affected by experimental conditions, which determine diffusion and charge transfer limitations at the electrodes [18].

EIS is considered as a more accurate method for analyzing bio-electrochemical reactions on electrodes, estimating electrode properties, and conducting mass transfer studies [8]. Several studies have used EIS to study MFC internal resistance, material influence, biofilm development, the effect of mediators, and bacteria immobilization on electrodes [8, 10, 13, 19–22]. Also, the CV technique

has been used in several MFC studies [22–26] for research on bacterial redox behavior and for electrochemical activity characterization of pure cultures and microbial consortia. By varying the electrode potential (E) at various scan rates and monitoring the resulting current, CV provides information about charge transfer at the biofilm—anode interface [9].

In this study, the development of the anodic biofilm was observed using a combination of the electrochemical techniques and measurements of the protein content of the anode.

2 Materials and methods

2.1 MFC design and operation

Five single-chamber membraneless air-cathode MFCs were operated for time periods ranging from 1 to 3 months. MFCs were assembled using polycarbonate plates and with a 50-mL anodic chamber (10 × 5 × 1 cm). A detailed description of the MFC design can be found in Martin et al. [14]. Anodes were made of 5 × 10 cm carbon felt with a thickness of 5 mm (Speer Canada, Kitchener, ON, Canada). Cathodes were made of carbon cloth gas diffusion electrodes with a Pt loading of 0.5 mg cm^{-2} (E-TEK division, PEMEAS Fuel Cell Technologies, Somerset, NJ, USA). The electrodes were separated with a J-cloth® so that the distance between them was approximately 1 mm. MFC voltage was measured using a data acquisition card (LabJack U12, LabJack Corp., Colorado, USA).

MFCs were operated at room temperature (22–24 °C) with no pH adjustment, which remained close to pH 7. A continuous flow mode with a hydraulic retention time of 12 h was used. External recirculation lines with peristaltic pumps were used for anodic liquid mixing. A concentrated solution of sodium acetate and nutrients, and dilution water were fed using a syringe pump (model NE-1000, New Era Pump Systems, Inc., Wantagh, NY, USA), and a peristaltic pump (Cole-Parmer Canada, Montreal, Canada), respectively. An influent acetate concentration of 2 g L^{-1} (corresponding to an acetate load of 4 g L_R day^{-1}) was maintained.

Based on the previous experimental results [14], all MFCs were started using a 400 Ω external resistance (R_{ext}). In the second phase of the experiment, R_{ext} of MFC1, MFC2, and MFC5 were step-wise decreased every 2–5 days to 100, 50, 30 Ω and then to 15 Ω (fast R_{ext} adjustment) to rapidly approach the estimated values of R_{int}. Then, these MFCs were operated at $R_{ext} \sim R_{int}$ to maximize power output according to Jacobi's law (maximum power transfer theorem). R_{ext} of MFC3 and MFC4 were decreased every 7–20 days (slow R_{ext} change) so that more than 2 months were required to approach R_{int} values. Consequently, these MFCs were operated at $R_{ext} \gg R_{int}$. Electrochemical measurements were carried out before each change of R_{ext}.

2.2 Inoculum, media composition, and analytical methods

The anodic compartments of the MFCs were inoculated with homogenized anaerobic mesophilic sludge with a volatile suspended solids content of 45–55 g L^{-1} (A. Lassonde Inc., Rougemont, QC, Canada). The stock solution of acetate and nutrients contained (in g L^{-1}): anhydrous sodium acetate (54.67), yeast extract (0.83), NH_4Cl (18.68), KCl (148.09), K_2HPO_4 (64.04), KH_2PO_4 (40.69). Acetate concentration in effluent was measured by gas chromatography (GC) using an Agilent 6890 (Wilmington, DE) with a detection limit of 0.2 mg L^{-1}. More details are provided in [14].

2.3 Protein measurements

To measure the protein concentration 1 × 1 × 0.5 cm pieces of carbon felt were taken from MFC5 anode on 4, 8, 11, 16, and 19 days after inoculation and were put into 2 mL tubes with 500 mg of 0.1 and 0.5 mm glass beads (zirconia/silica beads, Biospec Products, Inc., Bartlesville, OK, USA). The tubes were then filled with distilled water, vortexed to mix the beads and anode pieces, and then bead-beaten twice for 15 s using FastPrep® system (Bio 101 Savant, Bio/Can Scientific, Missisauga, Ontario, Canada). Subsequently, the samples were centrifuged, and the supernatant was collected and concentrated in a DNA concentrator (Savant DNA120 SpeedVac® concentrator, Thermo Fisher Scientific, Asheville, NC). The samples were then analyzed using the Bio-Rad protein assay protocol (Bio-Rad Laboratories Ltd., Mississauga, Ontario, Canada).

2.4 Electrochemical measurements

The testing procedure consisted of EIS measurements at working anodic potential (V_{app}), followed by open circuit monitoring for 1 h before carrying out cyclic voltammetry at various scan rates. The MFCs were then left in open circuit mode again for 1 h before performing polarization tests.

EIS was carried out using a frequency response analyzer (FRA) (model 1260A, Solartron Analytical, Hampshire, UK) connected to a potentiostat (Solartron 1470, Solartron Analytical, Hampshire, UK). ZPlot and ZView software (Solartron Analytical, Hampshire, UK) were used for instruments control and data analysis, respectively. The

experiments were done in a three-electrode mode using an Ag/AgCl reference electrode (1 M KCl, 222 mV vs NHE), the anode as a working electrode and the cathode as a counter electrode. The measurements were performed at the anode working potential while MFCs were operated at constant external resistance (R_{ext}). EIS tests were performed at an AC signal amplitude of 5 mV, at 37 logarithmic frequency steps between 100 kHz and 5 mHz. The test duration was approximately 30 min.

Acquired EIS spectra were described using a two time-constant model shown in Fig. 1, where R_S is the solution resistance, R^{oth} is the resistance of a secondary redox process, CPE^{oth} is its constant phase element, R_A^{ct} is the anodic charge transfer resistance for substrate oxidation, and CPE^{ct} is the constant phase element related to charge transfer. Constant phase elements are used instead of standard capacitances in this model because of inhomogeneous conditions (roughness, porosity, and distribution of reaction sites) [27]. Fitting both semi-circles with a CPE permits to obtain surface capacitance and influence of diffusion and electrode structure.

CV was performed using a potentiostat (273A, Princeton Applied Research, Tennessee, USA). The anode and cathode were used as working and counter electrodes respectively. A 1 M Ag/AgCl reference electrode was also used. Voltammetry was carried out at scan rates between 5 and 300 mV s^{-1} and at amplitudes between −0.9 and 0.4 V (vs Ag/AgCl). CorrWare and CorrView software (Solartron Analytical, Hampshire, UK) were used for potentiostat control and data analysis, respectively.

Polarization tests were carried out using a potentiostat (273A, Princeton Applied Research, Tennessee, USA), which controlled the cell voltage (E_{MFC}) while measuring the generated current (I). The tests were performed starting from OCV to short-circuit voltage at a scan rate of 0.5 mV s^{-1}. The MFC anode (carbon felt) was employed as a working electrode and the MFC cathode was used as a counter and reference electrode. Also, electrode potentials were measured against Ag/AgCl reference electrodes using a data acquisition card (LabJack U12, LabJack Corporation, Colorado, USA). The measurements were used to evaluate MFC internal resistance (R_{int}) and maximum power output (P_{max}). Anode and cathode potentials were also plotted against current to estimate anode and cathode resistances (R_A and R_C, respectively) from the linear parts of the curves.

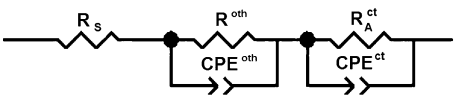

Fig. 1 A two time-constant model

Apparent Coulombic efficiency (CE_A) was calculated using measured current and the amount of acetate consumed in the MFC. This calculation does not account for the amount of acetate consumed by acetoclastic methanogens [14]. The removal efficiency (E_{Ac}) was evaluated by calculating the acetate removal according to the following equation:

$$E_{Ac} = \frac{M_{in} - M_{out}}{M_{in}} \times 100\% = \frac{(F_{in} \times C_{stock}) - (F_{out} \times C_{out})}{(F_{in} \times C_{stock})} \times 100\% \quad (1)$$

where F_{in} and F_{out} are, respectively, the stock solution and the effluent flow rates (L s^{-1}), and C_{stock} and C_{out} are acetate concentration in stock solution and acetate concentration in effluent (g L^{-1}).

3 Results and discussion

The evolution of internal resistances (R_{int}, R_A, R_C), OCV, and maximal power outputs (P_{max}) over time was observed through polarization tests. During the first 5–7 days of operation, the output voltage remained below 50 mV for all MFCs. Nevertheless, in all MFCs the polarization tests revealed a progressive increase of OCV to 530–600 mV and decrease of R_{int} from more than 2,500 Ω at start up to 450–500 Ω after the first 11 days. Estimations of R_A using electrode potential measurements against the Ag/AgCl reference electrode suggested that these changes were due to the proliferation of anode-reducing microorganisms at the anodes, as the anode open circuit potential became more negative (Fig. 2) and R_A decreased (Tables 1, 2). On average R_A decreased from about 2,000 to 200-400 Ω. In all MFCs, the anode potential corresponding to maximum power output became more negative with time approaching ∼ −380 mV versus Ag/AgCl electrode at maximum power generation (Fig. 2). This observation agrees with other studies [28, 29], where a maximum of electrogenic activity was observed at anodic potentials between −300 and −420 mV versus Ag/AgCl.

The observed changes of the anode potential and internal resistance were indicative of the electrode colonization by the anode-reducing microorganisms. Samples of MFC5 carbon felt anode were periodically taken to measure the concentration of proteins to follow biofilm formation. Notably, anode sampling required periodic exposure of the anodic compartment to air and decreased the anode size after each sampling. Since such sampling procedure could affect the electrochemical characteristics of the anode, MFC5 was not used for CV and EIS tests. Measurements of the protein content of the MFC5 anode showed increasing

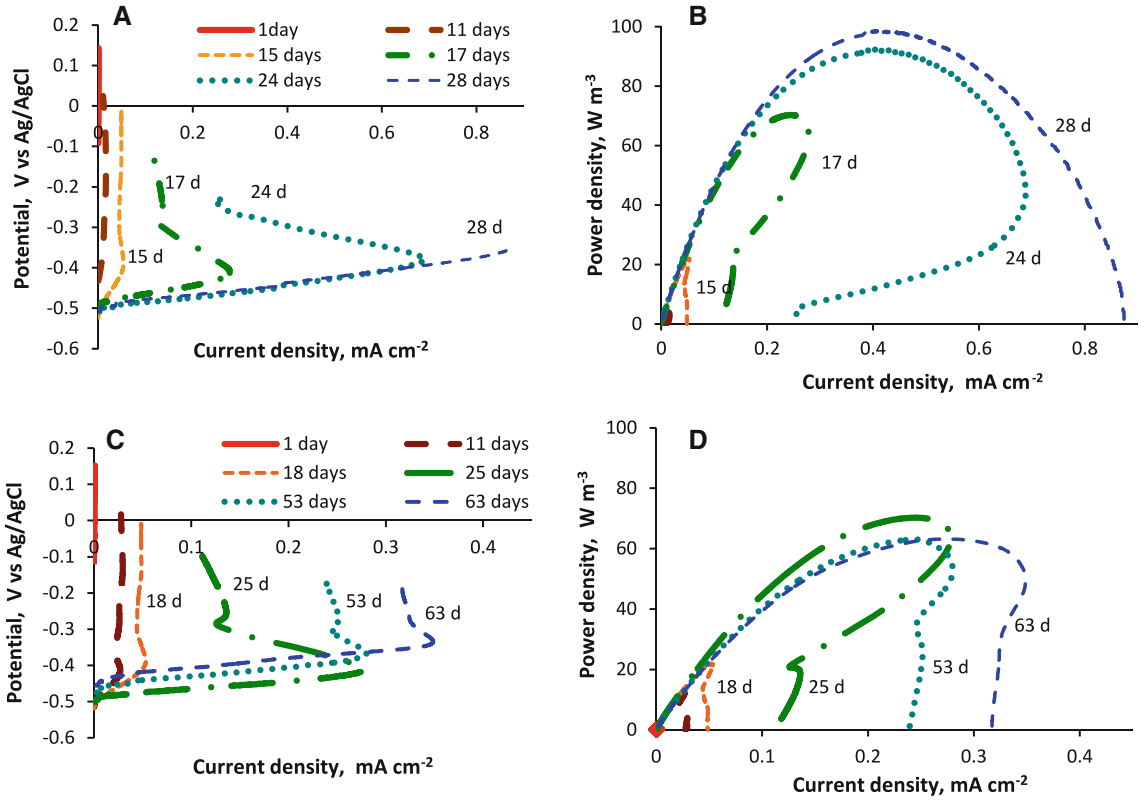

Fig. 2 Time-related changes in the anode polarization (**a**, **c**) and power (**b**, **d**) curves observed in MFC2 operated at $R_{ext} \sim R_{int}$ (**a**, **b**) and in MFC4 operated at $R_{ext} > R_{int}$ (**c**, **d**)

Table 1 Characterization of MFC1 and MFC2 operated with a fast adjustment of R_{ext} resulting in $R_{ext} \sim R_{int}$

Days after inoculation	R_{ext} (Ω)	Acetate removal (%)	Coulombic efficiency (%)	Polarization tests			EIS tests	
				P_{max} (W m^{-3})	R_{int} (Ω)	R_{anode} (Ω)	R^{ct} (Ω)	R_{anode} total (Ω)
4	400	66.1	0.9	1.4	728.9	529.1	665.3	666.0
11	400	71.3	1.7	4.2	433.1	207.3	245.7	247.0
15	400	73.9	4.9	13.3	86.8	32.4	18.4	19.8
17	100	83.2	13.5	36.2	37	9.6	6.5	7.9
11 and 22	50	90.4	24.1	79.4	14.1	4.4	3.7 ± 0.9	5.0 ± 0.8
24	30	90.9	32.9	77.3 ± 15.1	18.9 ± 7.6	7.6 ± 4.6	2.6	4.3
28	15	93.9	48.1	98.6	10.7	3	1.9	3.7

protein concentration with time suggesting biofilm development at the anode (Fig. 3a). Also, scanning electron micrographs confirmed biofilm formation around the carbon felt anode fibers (results not shown). The observed increase of the protein concentration coincided with the continuing improvement of MFC performance expressed as MFC current density in Fig. 3a. Also, acetate removal and coulombic efficiencies increased with time reaching 94 and 48 %, respectively (Table 1). This evolution in MFC performance agrees with the increasing density of the electrode-reducing microorganisms, as internal resistance is known to be linked to the catalyst load [30].

The strategy of fast R_{ext} adjustment to approach R_{int} led to higher power outputs and a faster decrease of R_A in MFC1 and MFC2 as compared to MFC3 and MFC4, which were operated at $R_{ext} >> R_{int}$ (Fig. 2; Tables 1, 2). We hypothesize that by operating MFCs at R_{ext} values close to R_{int}, electron transfer to the anode was facilitated by increasing its potential. These conditions facilitated either growth or activity of the anode-reducing microorganisms competing with acetoclastic methanogens for common carbon source (acetate). Eventually, MFC performance was improved due to the increased density of the anodophilic biofilm, which agrees with the results obtained in other

Table 2 Characterization of MFC3 and MFC4 operated with a slow adjustment of R_{ext} resulting in $R_{ext} >> R_{int}$

Days after inoculation	R_{ext} (Ω)	Acetate removal (%)	Coulombic efficiency (%)	Polarization tests			EIS tests	
				P_{max} (W m^{-3})	R_{int} (Ω)	R_{anode} (Ω)	R^{ct} (Ω)	R_{anode} total (Ω)
1 and 4	400	47.5 ± 9.0	0.3 ± 0.2	0.5 ± 0.3	2502 ± 1618	1975 ± 1385	1832 ± 217	1835 ± 219
8 and 11	400	47.8 ± 18.4	4.2 ± 1.2	11.2 ± 7.0	488.2 ± 27.7	377 ± 11.6	1539 ± 53	1549 ± 62
18 and 22	400	37.9 ± 16.1	11.1 ± 5.7	23.6 ± 1.9	64.1 ± 9.0	32.4 ± 2.0	14.2 ± 2.6	15.0 ± 2.5
25 and 35	100	53.7 ± 14.3	25.1 ± 7.1	49.2 ± 20.9	38.7 ± 16.5	13.6 ± 9.2	4.8 ± 2.3	5.9 ± 2.3
32 and 53	50	57.8 ± 18.1	39.8 ± 9.2	49.6 ± 20.5	36.0 ± 15.0	9.2 ± 5.8	4.7 ± 3.2	5.8 ± 3.1
53 and 57	30	57.3 ± 12.8	44.4 ± 1.3	62.9	20.5	5.1	1.7	3.1
63	15	63.7	77.8	63.1	19.1	5.2	1.9	3.1

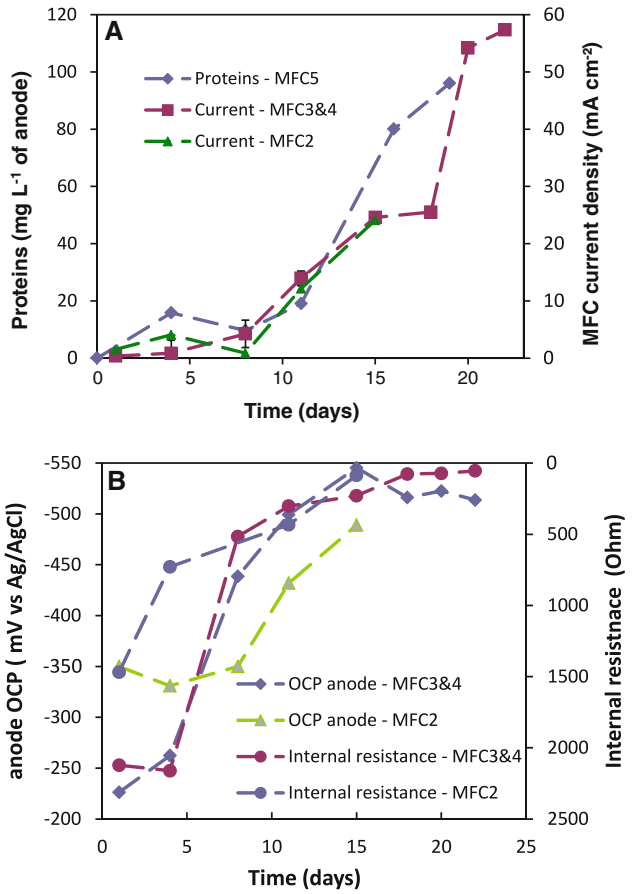

Fig. 3 **a** Measurements of time-related evolution of protein concentration at the anode and current density; **b** anode OCP and R_{int} measurements. MFC2 and MFC5 were operated at $R_{ext} \sim R_{int}$. While MFC3 and MFC4 were operated at $R_{ext} > R_{int}$

experimental studies [6, 31] and simulations of a two-population anodophilic-methanogenic microbial consortium [32].

Analysis of power curves in Fig. 2 showed that both MFC2 and MFC4 exhibited power overshoots during the first 24 days of operation. However, the overshoot disappeared in MFC2 polarization test performed on 28 day, while it was still present in MFC4 polarization tests (53 and 63 days in Fig. 2d). The phenomenon of power overshoot is often attributed to charge transfer limitations [33]. A comparison of power curves shown in Fig. 2 agrees with the results of the EIS tests described below suggesting that long-term MFC operation at $R_{ext} \sim R_{int}$ reduces charge transfer limitations. MFC operation at $R_{ext} \sim R_{int}$ has been used in several recent studies to maximize power production [11, 34, 35].

Although by the end of the experiment R_{int} and R_A values were not significantly different for all MFCs, the power output of MFC1 and MFC2 remained higher. Overall, the polarization tests showed that R_{int} and R_A decreased to 10–20 and 3–5 Ω, respectively. This observation suggests that MFC performance, although linked to biofilm density, might be also influenced by the microbial community structure, which is not only time-dependent, but is also affected by the external resistance chosen for MFC operation [5, 15, 19].

Estimations of the anodic resistance using the linear part of the polarization curves can be biased due to the influence of the reactants flow toward the electrode, (i.e., diffusion and charge transfer limitations are included) and the existence of additional redox processes. Consequently, EIS measurements were carried out to validate the R_A estimations obtained in the PTs. Impedance studies of MFCs with carbon felt anodes often use a one time-constant model for resistance estimation [8, 10, 13, 19, 21]. However, the initial analysis of the EIS spectra showed the presence of two semi-circles in MFC1-MFC4 spectra (Fig. 4), thus necessitating the use of the two time-constant model shown in Fig. 1. The existence of two semi-circles in EIS spectra of MFCs was also noticed by Ramasamy et al. [20], who suggested that the high frequency semi-circle is caused by endogenously produced redox mediators used as a shuttle for electron transfer and metallic salts oxidation or reduction on anodes. To verify this hypothesis, EIS measurements were carried out in a MFC filled with the solution of nutrients and microelements used during MFC operation

but containing no biomass. This abiotic test showed a high frequency semi-circle corresponding to the first semi-circle in Fig. 4, while the second semi-circle was absent. The width of the high frequency semi-circle in the abiotic test was only slightly smaller as compared to MFCs with the anode-reducing microorganisms. Thus, the presence of the high frequency semi-circle in our tests could be attributed to salts of the influent solution (e.g., phosphates) rather than endogenous mediators.

Overall, EIS measurements confirmed R_A trends obtained in the polarization tests. It also showed the decrease in charge transfer resistance (R^{ct}) with time (Tables 1, 2). R_A values estimated by the two methods were in a reasonable agreement, although values obtained in polarization tests tended to be higher, at least at the beginning of biofilm formation when the R_A was high. Interestingly, EIS measurements revealed an increase in MFC capacitance on average from 79 ± 38 mF measured after first 2 weeks of MFC operation to 440 ± 272 mF by the end of the test. The capacitance measured at the end of the experimental period was similar to values reported for a mature biofilm in another study [19]. The considerable capacitance increase indicates a larger active surface area and an increase of the active reaction sites. This suggests an increase in anode colonization by anode-reducing microorganisms rather than an increase in the microbial activity of a near constant number of microorganisms. The CPE used for fitting provided, along with the capacitance estimation, an indication of the significant influence of the electrode inhomogeneity on anodic charge transfer, rather than diffusion processes [10, 19, 21].

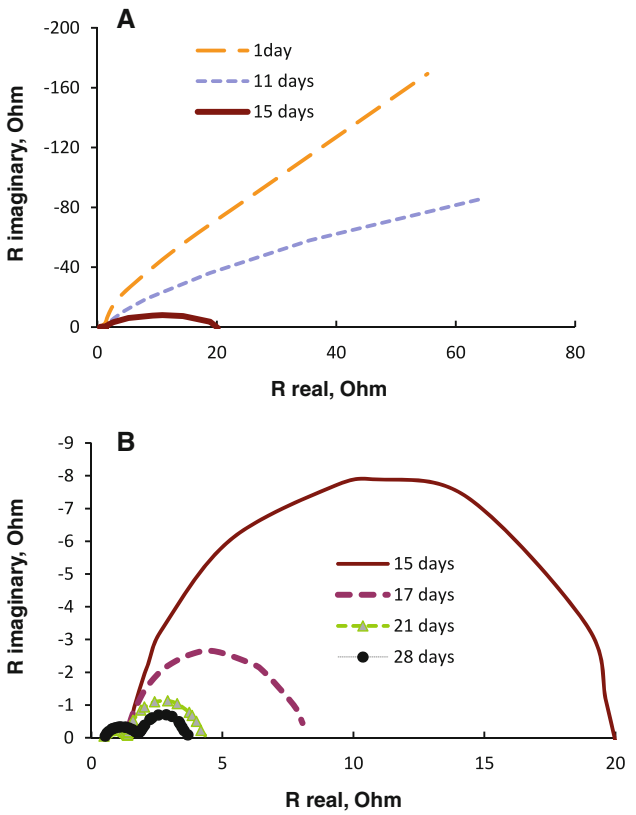

Fig. 4 Anode EIS spectra observed during **a** 0–15 days; and **b** 15–28 days of MFC2 operation

The evolution of the anode cyclic voltammograms over time provided another valuable monitoring tool showing the appearance of redox peaks at potentials around −330 and −170 mV (vs Ag/AgCl electrode) shortly after MFC start up and before the increase in output voltage was observed around 5–7 days (Fig. 5). Voltammograms of MFC1 and MFC2 showed that simultaneously with the voltage increase, the redox system located at −330 mV intensified, while the redox system at −170 mV either remained unchanged or appeared to merge with the redox system at −330 mV (Fig. 5a). CVs of MFC3 and MFC4 where R_{ext} remained above R_{int} showed that the redox system at −330 mV was predominant (Fig. 5b). Voltammograms of all MFCs showed increased current generated by the oxidation reaction with time as can be seen from the evolution of the normalized current density corresponding to the current peak at around −330 mV (Fig. 6). Once again, this pointed to the proliferation of the anode-reducing microorganisms.

The presence of multiple redox systems indicates that more than one oxidation–reduction reaction of biological matter can occur at the anode surface. Based on these results, we hypothesized that more than one electroactive species (microorganisms or mediators) could be responsible for charge transfer, although only one of them was predominant. Also, it appeared that the presence of the two redox systems in the MFCs operated at $R_{ext} \sim R_{int}$ resulted in a higher power output. Indeed, anaerobic sludge contains a diverse microbial population capable of electron transfer using different charge transfer mechanisms (e.g., through cytochrome-based and mediated transfer) as described by Aelterman [6]. Notably, mediated transfer is possible in multiple ways and through several mediators (quinones, phenazines, melanin, flavins, and metal chelates) [1, 3, 36, 37]. The co-existence of these mediators cannot be excluded. Biofilms that develop on anodes of such systems are likely to be important environments for metabolisms that employ extracellular electron transfer, since electron shuttling has been reported for several different bacterial species and exchanges of shuttling compounds (syntrophy) most likely occurs in such biofilms [2, 37].

Previous works pointed out the possibility of multiple steps of charge transfer by *Geobacter* sp. [24, 25], while a recent study proposed electron transfer paths for *Geobacter* that consist of outer membrane electrode-bound cytochromes working as a series of mediators with different redox potentials [26]. Therefore, it can be hypothesized

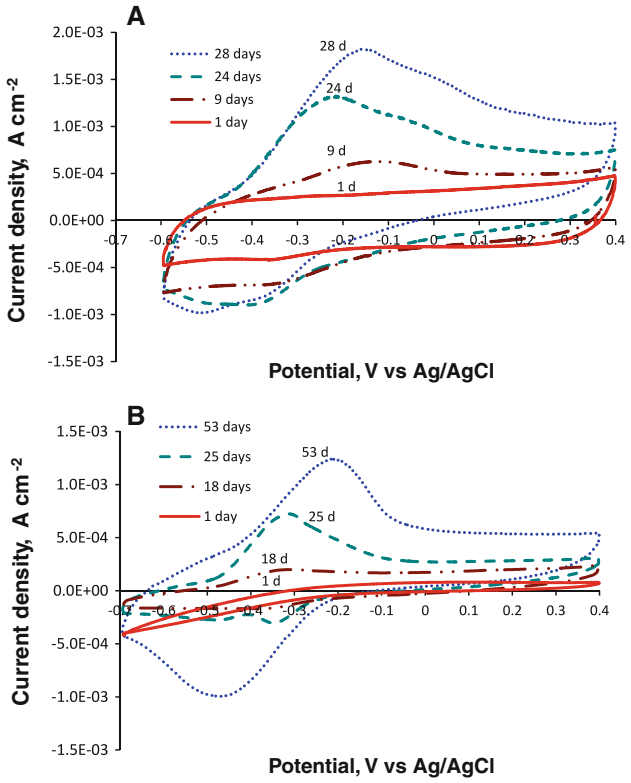

Fig. 5 Time-related evolution of the anode cyclic voltammograms observed during MFC2 ($R_{ext} \sim R_{int}$) **a** and MFC4 ($R_{ext} > R_{int}$) **b** operation. CVs were acquired at a scan rate of 100 mV s^{-1}

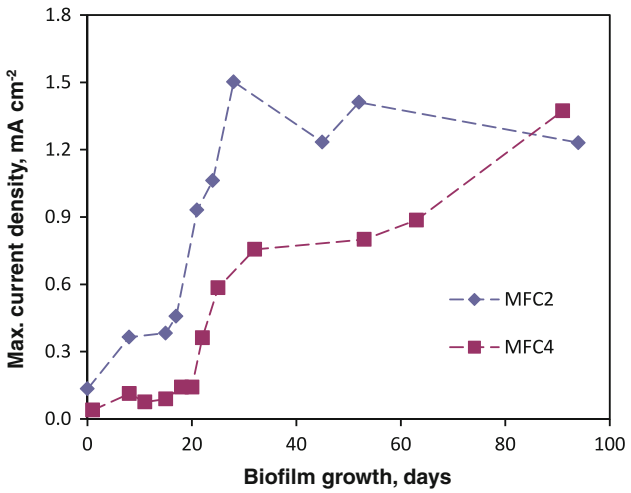

Fig. 6 Anodic peak current density ($i_{p.a}$) acquired during CV tests at 50 mV s^{-1} for MFC2 operated at $R_{ext} \sim R_{int}$ and MFC4 operated at $R_{ext} > R_{int}$

that in addition to the existence of several electrochemically active species, the charge transfer pathway may vary depending on MFC operating conditions and the microorganism distance from the anode.

Further electrochemical characterization was carried out by conducting CVs at several scanning rates and plotting normalized anodic peak current densities ($I_{p,a}/ I_{p,a,min}$) against the scan rate (ν). The tests conducted at several biofilm development phases showed that the normalized current density of the redox peak at around −330 mV is linearly proportional to the square root of ν. Similar dependence on ν was obtained in MFCs operated at low and high values of R_{ext}. An example of this behavior observed during MFC4 operation is shown in Fig. 7. This suggests that the charge transfer process became diffusion limited [24, 26]. Also, $I_{p,a}$ increase with ν indicates a partially diffusion-controlled process, but not an irreversible diffusion-controlled process [38]. The slopes of the curves decrease with increasing biofilm development time and this decrease was more pronounced in MFCs operated at a high R_{ext}. Thus, diffusion limitation due to the increasing amount of microorganisms was significant in all MFCs. However, MFC operation at a higher R_{ext} apparently resulted in a biofilm with a higher diffusion limitation as compared to a lower R_{ext}, tested in MFC2 (results not shown), possibly due to a significant number of non-anode-reducing microorganisms, e.g., methanogens, growing at the carbon fiber surface. Also, MFC operation at high values of R_{ext} slowed the development of the anode-reducing microorganisms so that significantly longer times were required to form a mature conductive biofilm matrix.

4 Conclusion

Through the application of multiple electrochemical techniques, this study demonstrated the dynamics of the anodophilic biofilm formation. We observed the evolution of the anodic microbial population with time and

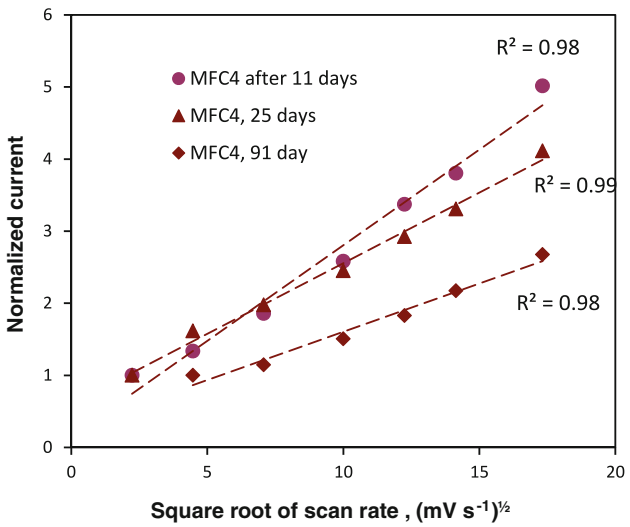

Fig. 7 Dependence of the normalized anodic peak current density (i/i_{min}) on the square root of the scan rate measured during MFC4 test ($R_{ext} > R_{int}$)

demonstrated the effect of biofilm development on the anode internal resistance and open circuit potential. Interestingly, the dynamics of the anodophilic biofilm formation was dependent on MFC external resistance. MFCs operated at R_{ext} close to R_{int} not only featured a higher power output and a lower internal resistance, but also showed differences in the observed redox reactions. Although a redox couple at −330 mV was predominant in all MFCs, the MFCs with a higher power output featured the presence of a second redox couple, albeit with a smaller peak area. We hypothesize that the best efficiency in MFCs can be achieved by combining several charge transfer mechanisms and that MFC operation at R_{ext} close to its R_{int} value promotes the growth of several electrode-reducing microorganisms.

Acknowledgments Assistance of Punita Mehta in performing protein analysis is greatly appreciated. Funding for this study was provided by NSERC and NRC Canada.

References

1. Schroder U (2007) Phys Chem Chem Phys 9:2619–2629
2. Lovley DR (2008) Curr Opin Biotechnol 19:564–571
3. Torres CI, Marcus AK, Lee H-S, Parameswaran P, Krajmalnik-Brown R, Rittmann BE (2009) FEMS Microbiol Rev 34:3–17
4. Franks AE, Malvankar N, Nevin KP (2010) Biofuels 1:589–604
5. Kiely P, Call D, Yates M, Regan J, Logan B (2010) Appl Microbiol Biotechnol 88:371–380
6. Aelterman P, Versichele M, Marzorati M, Boon N, Verstraete W (2008) Bioresour Technol 99:8895–8902
7. Borole AP, Hamilton CY, Vishnivetskaya T, Leak D, Andras C (2009) Biochem Eng J 48:71–80
8. He Z, Mansfeld F (2009) Energy Environ Sci 2:215–219
9. Logan BE, Hamelers B, Rozendal R, Schroder U, Keller J, Freguia S, Aelterman P, Verstraete W, Rabaey K (2006) Environ Sci Technol 40:5181–5192
10. Manohar AK, Bretschger O, Nealson KH, Mansfeld F (2008) Bioelectrochemistry 72:149–154
11. Aelterman P, Versichele M, Marzorati M, Boon N, Verstraete W (2008) Biores Technol 99:8895–8902
12. Pei-Yuan Z, Zhong-Liang L (2010) J Power Sources 195: 8013–8018
13. Manohar AK, Mansfeld F (2009) Electrochim Acta 54:1664–1670
14. Martin E, Savadogo O, Guiot SR, Tartakovsky B (2010) Biochem Eng J 51:132–139
15. Lyon DY, Buret F, Vogel TM, Monier J-M (2010) Bioelectrochemistry 78:2–7
16. Li X, Hub B, Suibb S, Lei Y, Li B (2011) Biochem Eng J 54:10–15
17. Clauwaert P, Aelterman P, Pham T, De Schamphelaire L, Carballa M, Rabaey K, Verstraete W (2008) Appl Microbiol Biotechnol 79:901–913
18. Flandin L, Danerol AS, Bas C, Claude E, De-Moor G, Alberola N (2009) J Electrochem Soc 156:B1117–B1123
19. Borole AP, Aaron D, Hamilton CY, Tsouris C (2010) Environ Sci Technol 44:2740–2745
20. Ramasamy RP, Gadhamshetty V, Nadeau LJ, Johnson GR (2009) Biotechnol Bioeng 104:882–891
21. Ramasamy RP, Ren Z, Mench MM, Regan JM (2008) Biotechnol Bioeng 101:101–108
22. Srikanth S, Marsili E, Flickinger MC, Bond DR (2008) Biotechnol Bioeng 99:1065–1073
23. Chung K, Okabe S (2009) Appl Microbiol Biotechnol 83: 965–977
24. Fricke K, Harnisch F, Schroder U (2008) Energy Environ Sci 1:144–147
25. Liu Y, Harnisch F, Fricke K, Schröder U, Climent V, Feliu JM (2010) Biosens Bioelectron 25:2167–2171
26. Richter H, Nevin KP, Jia H, Lowy DA, Lovley DR, Tender LM (2009) Energy Environ Sci 2:506–516
27. Barsoukov E, Macdonald JR (2005) Impedance spectroscopy—theory, experiment, and applications. Wiley, Hoboken
28. Torres CI, Marcus AK, Rittmann BE (2008)). Biotechnol Bioeng 100:872–881
29. Cheng KY, Ho G, Cord-Ruwisch R (2008) Environ Sci Technol 42:3828–3834
30. Chaparro AM, Gallardo B, Folgado MA, Martín AJ, Daza L (2009) Catal Today 143:237–241
31. Freguia S, Rabaey K, Yuan Z, Keller J (2007) Environ Sci Technol 41:2915–2921
32. Pinto RP, Srinivasan B, Manuel M-F, Tartakovsky B (2010) Bioresource Technol 101:5256–5265
33. Watson VJ, Logan BE (2011) Electrochem Commun 13:54–56
34. Grondin F, Perrier M, Tartakovsky B (2012) J Power Sources 208:18–23
35. Premier GC, Kim JR, Michie I, Dinsdale RM, Guwy AJ (2011) J Power Sources 196:2013–2019
36. Debabov V (2008) Microbiology 77:123–131
37. Hernandez ME, Newman DK (2001) Cell Mol Life Sci 58:1562–1571
38. Bard AJ, Faulkner LR (2001) Electrochemical methods: fundamentals and applications. Wiley, Toronto